RESEARCH REPORTS
Biomaterials & Bioengineering

S.N. White[1*,2], W. Luo[1], M.L. Paine[1], H. Fong[3], M. Sarikaya[3], and M.L. Snead[1]

[1]Center for Craniofacial Molecular Biology, University of Southern California School of Dentistry, CSA 103, 2250 Alcazar Street, Los Angeles, CA 90033; [2]School of Dentistry, UCLA, Los Angeles, CA 90095; [3]Department of Materials Science and Engineering, University of Washington, Seattle, WA 98195; *corresponding author, snwhite@ucla.edu

J Dent Res 80(1):321-326, 2001

Biological Organization of Hydroxyapatite Crystallites into a Fibrous Continuum Toughens and Controls Anisotropy in Human Enamel

ABSTRACT

Enamel forms the outer surface of teeth, which are of complex shape and are loaded in a multitude of ways during function. Enamel has previously been assumed to be formed from discrete rods and to be markedly aniostropic, but marked anisotropy might be expected to lead to frequent fracture. Since frequent fracture is not observed, we measured enamel organization using histology, imaging, and fracture mechanics modalities, and compared enamel with crystalline hydroxyapatite (Hap), its major component. Enamel was approximately three times tougher than geologic Hap, demonstrating the critical importance of biological manufacturing. Only modest levels of enamel anisotropy were discerned; rather, our measurements suggest that enamel is a composite ceramic with the crystallites oriented in a complex three-dimensional continuum. Geologic apatite crystals are much harder than enamel, suggesting that inclusion of biological contaminants, such as protein, influences the properties of enamel. Based on our findings, we propose a new structural model.

KEY WORDS: tooth, enamel, microstructure, organization, toughness.

INTRODUCTION

Dental enamel is a composite bioceramic composed largely of hydroxyapatite (Hap) and small amounts of proteins. Human enamel rarely undergoes catastrophic mechanical failure despite a lifetime of repeated masticatory, parafunctional, and occasional impact loading.

Most theoretical mechanical models of enamel have assumed that enamel behaves in a highly anisotropic manner (Yettram *et al.*, 1976; Spears *et al.*, 1993). This assumption is based on prior models of enamel structure that are composed of discrete and mostly parallel rods. However, the structural organization of enamel remains controversial, as evidenced by many published conference discussions (*e.g.*, Boyde, 1979, 1997). For the presentation of the data in this current study, the terms rod and interrod will be used. The assumption of anisotropy is supported by some experimental evidence (Rasmussen *et al.*, 1976; Hassan *et al.*, 1981; Xu *et al.*, 1998). However, teeth are of complex shape and are loaded in a multitude of ways during function, so marked anisotropy might be expected to lead to undue fracture.

The functional success of enamel is also somewhat surprising, given that it is largely composed of weak and brittle Hap crystallites. Although the fracture toughness of crystalline Hap has not yet been reported, it is probably very low, certainly substantially lower than that of artificial materials currently used to replace missing enamel (Ashby, 1993; Lawn, 1993).

Since frequent fracture is not observed, we designed an experimental strategy to measure enamel biofabrication and spatial and biomechanical organization using histology, scanning electron microscopy (SEM), and fracture mechanics modalities. We propose that enamel is organized to form a tough complex continuum that resists crack propagation along as well as across the dominant rod direction, and that it is only moderately anisotropic.

MATERIALS & METHODS

Biofabrication, Histology

Human tissues were used in compliance with NIH guidelines. Incisor teeth from an aborted three-month-old human fetus were fixed in 1% paraformaldehyde, embedded, sectioned sagittally, and stained with 0.5% toluidine blue for morphologic evaluation or with von Kossa's method for evaluation of calcification.

Spatial Organization, SEM

Adult human incisor teeth were prepared for SEM by being ground in a sagittal plane and polished prior to being etched three times, for 30 sec each time, in 1% nitric acid and sputter-coated with gold-palladium (Risnes, 1998). The teeth were viewed in a SEM (Cambridge 360, Leo Electron Microscopy, Cambridge, UK) at 10 KV.

Biomechanical Organization, Fracture Mechanics

Ten adult human incisor teeth, kept moist at all times, were prepared as previously described (White *et al.*, 2000). A Vickers microhardness testing machine was used to make indentations at the center of the enamel thickness at

Received February 10, 2000; Last revision October 18, 2000; Accepted November 2, 2000

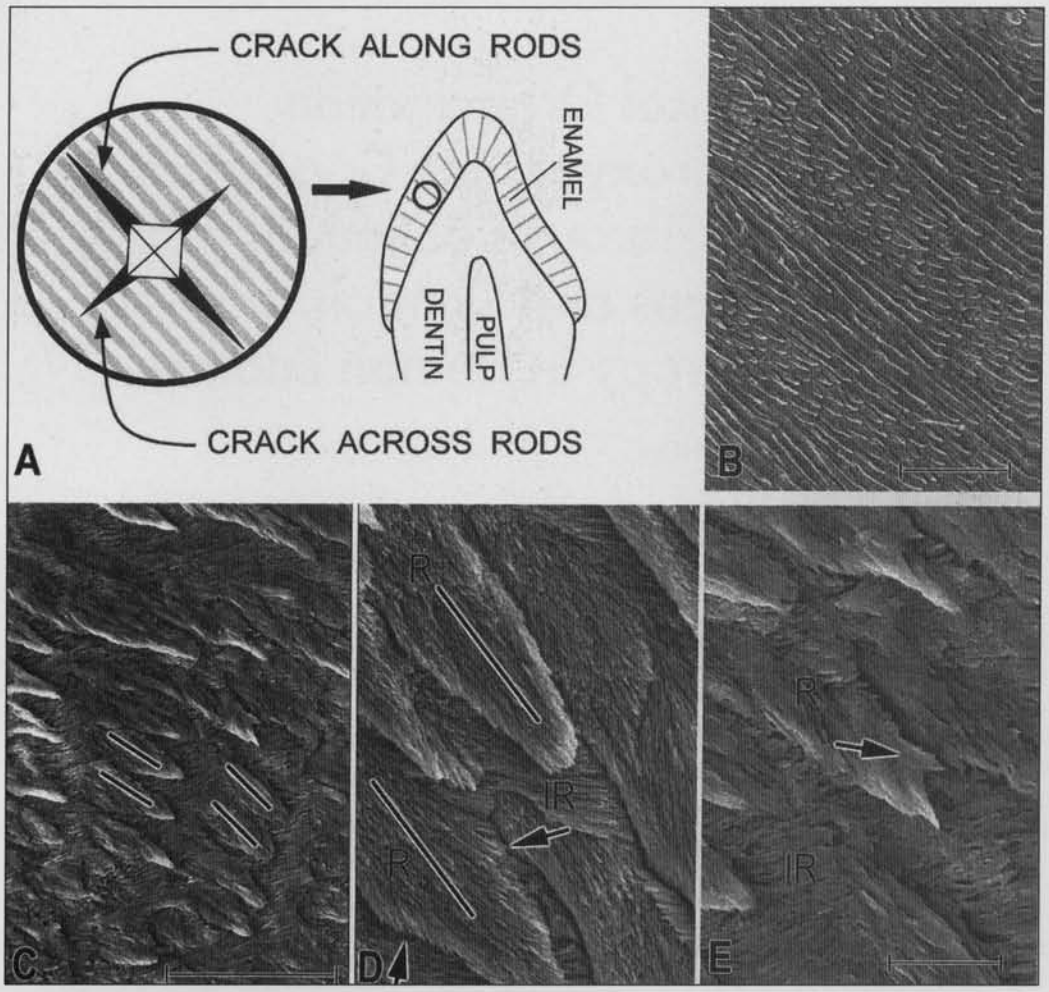

Figure 1. (A) Schematic diagram of Vickers indentation and location of indentation area in sagittally sectioned specimen. All Figs. are from the same area. Enamel rod orientation is indicated by gray lines. Indentations are oriented so that the radial cracks (black) extend across and along the rods. All panels in Figs. 1 and 2 are positioned and oriented as in this schematic. Panel **B** is a sagittal section SEM showing the large angle of decussation between Hunter-Schreger bands (cohorts of approximately 10 rods) (bar = 50 μm). Panel **C** shows the small angle of decussation between adjacent layers of rods within a single Hunter-Schreger band (bar = 20 μm). Lines indicate the orientation of adjacent layers of rods. Crystallites can be seen crossing from rod to rod at an angle of approximately 60° to the long axes of the rods. Panels **D** & **E** show SEMs of rod (R) and interrod (IR) in sagittal section (bar = 5 μm). Peripheral crystallites (arrows in Panel **D**) deviate from the long axes of the rods to form a continuum with interrod (arrow in Panel **E**). Interrod crystallites cross rods at an angle of approximately 60°.

the junction of the incisal third and the middle third of the facial enamel (Fig. 1). The indentations were spread apart at least 3 times their radial crack lengths. The specimens were oriented so that the radial cracks were oriented along and across the direction of the enamel rods (Fig. 1). A 500-g load and a dwell time of 20 sec were used. These indentations were used for calculation of both fracture toughness and hardness. Fracture toughness is an especially valuable parameter because the damage produced is specific to the substrate's intrinsic microstructure. Five repetitions were averaged to describe each of the 10 teeth. Overall means and standard deviations were calculated.

To evaluate the importance of the biological organization, we compared the fracture toughness of enamel with that of individual apatite crystals. Due to the extremely small size of dental Hap crystallites, it is currently not possible to measure their fracture toughness. Therefore, two types of geologic apatite crystal-Holley Springs Hap (Cherokee County, GA) and Durango fluorapatite (Cerro de Mercado, Durango, Mexico)-were compared with enamel. Crystallites in tooth enamel are not pure Hap, but are a carbonated form of hydroxyapatite, dahllite (Boyde, 1979; Lowenstam and Weiner, 1989). Fluorapatite differs from Hap in the substitution of fluorine ions for similarly sized hydroxyl ions within the crystal lattice and may have the potential to alter mechanical properties. Indentations were made on the 100 surfaces at an orientation parallel and perpendicular to the c axis of the geologic apatite crystals under moist conditions. A 100-g load and a dwell time of 20 sec were used. Five repetitions were averaged to describe 8 Hap and 8 fluorapatite crystals. Overall means and standard deviations were then calculated for fracture toughness and hardness.

Vickers hardness and fracture toughness were calculated in the customary manner (Xu *et al.*, 1998). The value used for the elastic modulus of enamel was 84 GPa (Craig *et al.*, 1961; Xu *et al.*, 1998). However, elastic modulus may vary with rod orientation. Since this has not yet been studied, 84 GPa was used for both across- and along-rod calculations. The value used for the elastic modulus of both fluorapatite and Hap was 119 GPa. This value was derived from a single ultrasonic study on Durango fluorapatite, but it seems reasonable in comparison with published values for other weak crystalline materials (Clark, 1966; Yoon and Newham, 1969; Ashby 1993; Lawn, 1993). The elastic modulus of a crystalline material may vary with orientation, but a single value was used.

Table. Mechanical Properties of Enamel, Hydroxyapatite, and Fluorapatite

	Fracture Toughness Mean and SD in $MPam^{1/2}$	Vickers Microhardness Mean and SD in GPa
Enamel along rods	0.90 (0.22)	-
Enamel across rods	1.30 (0.30)	-
Enamel	-	3.0 (0.7)
Holley Springs hydroxyapatite	0.37 (0.04)	5.4 (1.3)
Durango fluorapatite	0.39 (0.04)	5.1 (1.3)

RESULTS

Biofabrication, Histology

The stained histological sections (Fig. 2) show pronounced apical-incisal asymmetry in the shape of the apically oriented Tomes' process. The incisal surface of the Tomes' process is longer than the apical surface. The apically facing tip of the Tomes' process, where rod is formed, often appears flat or slightly concave. Interrod extends between adjacent Tomes' processes. Increased alizarin red staining of interrod suggests that it contains more calcium than adjacent rod; thus it initially mineralizes before adjacent rod.

Spatial Organization, SEM

At low magnification, the SEMs show that the human enamel contains Hunter-Schreger bands (Fig. 1B). Each band or cohort was composed of approximately 10 layers of rods. Each band or cohort had a large angle of decussation with adjacent cohorts. Within single bands or cohorts, adjacent layers of rods have a small angle of decussation (Fig. 1C). Therefore, human enamel has two separate levels of decussation.

At high magnification, the SEMs show crystallite orientation (Figs. 1, 2). Individual crystallites are approximately 100 nm in diameter. Rods are bundles of crystallites approximately 4.5 μm in diameter. Organization of crystallites was evident within rods, in rod-to-interrod connections, and within interrod.

In bulk enamel, rods are largely surrounded by interrod to produce the characteristic "honeycomb" appearance. Interrod takes the form of an undulating sheet of Hap crystallites approximately 0.5 μm thick (Figs. 1-3). Most of the crystallites within each rod run in a direction approximately parallel to the course of the rods. In contrast, the interrod crystallites are at an angle of approximately 60° to the long axes of the rods.

Face-on or surface views show that the incisal surface and the lateral sides of rods are typically rounded, clearly defined, and surrounded by a sheet of interrod (Figs. 2C, 3). However, the apical surfaces of rods are continuous with the interrod phase. Thus, rod and interrod form a single continuum. The incisal and lateral surfaces of the rods produce the outline of the characteristic "fish scale" appearance, but the apical surface or base of the "scale" is less well-defined and becomes continuous with interrod.

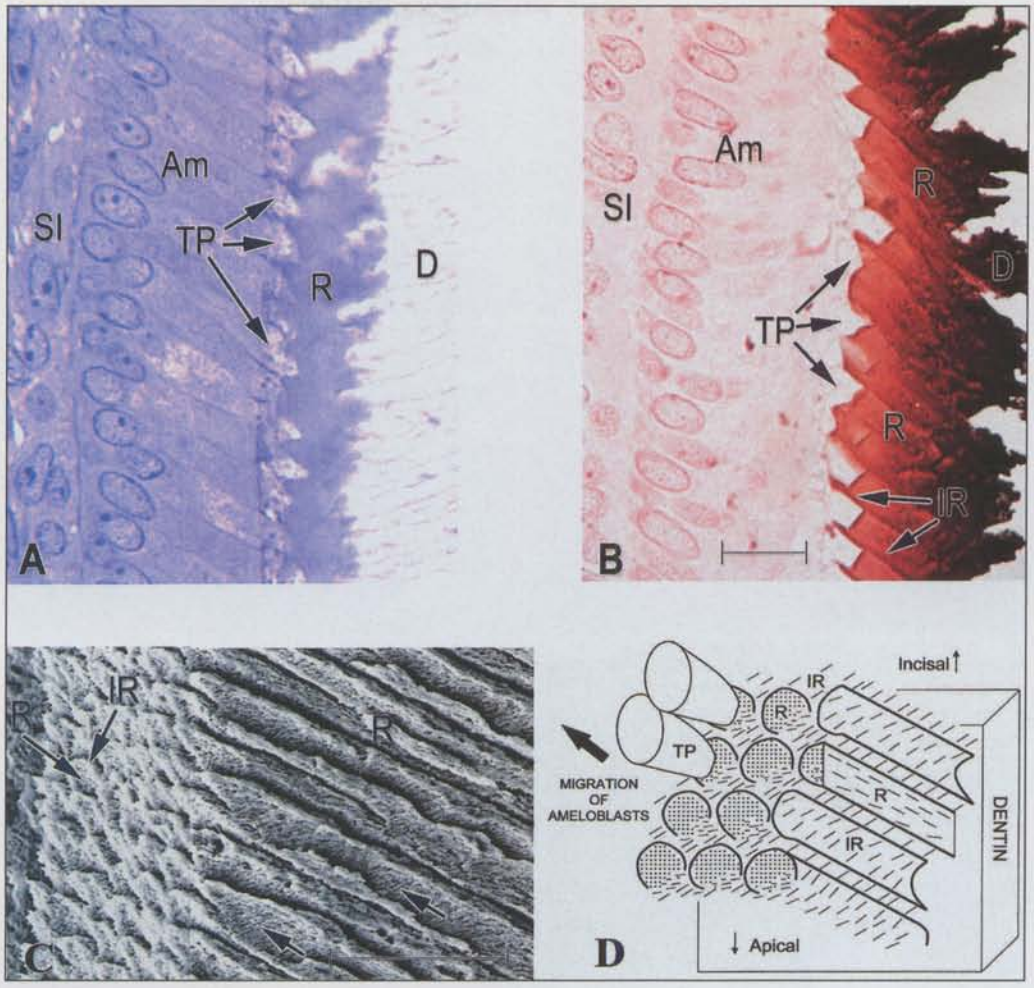

Figure 2. Panels **A** (toluidine blue stain) and **B** (von Kossa stain) show light micrographs of histologic sagittal sections of tooth organ (Am = ameloblasts, SI = stratum intermedium, D = dentin) (bar = 10 μm). Both micrographs show that the incisal surface of the Tomes' process (TP) is longer than the apical surface. Panel **B** shows deeper staining and more calcification of the earlier-forming interrod (IR) than of the later-forming rod (R). Interrod extends between adjacent Tomes' processes. The SEM in panel **C** shows both cross-sectional (outer facial surface) and long-sectional (sagittal) views of rod and interrod (bar = 20 μm). Rods are largely surrounded by distinct interrod, but the apical surface of each rod blends into interrod to form a continuum, producing the "fish scale" appearance. The presence of interrod crystallites running at approximately 60° to the long axis of the rods is especially evident, because the rod crystallites have been preferentially etched away (arrows). Panel **D** is a schematic of the proposed enamel microstructure model that includes several important points. First, the paths of the Tomes' processes create a "staggering" between adjacent layers of rod, governing the possible spatial and temporal relationships among forming rods, and their possible connections. Second, the orientation of the crystallites within rod and interrod is related to shape and orientation of the secretory sites of the Tomes' processes (TP) and the vectors of movement of the ameloblasts. Third, it appears that rod is primarily contributed by the basal tip of the Tomes' process, whereas interrod is contributed by the sides of the process, especially by the longer incisal surfaces. Fourth, the dominant rod and interrod crystallite orientations differ by an angle of approximately 60° in the sagittal plane. Fifth, boundaries or potential fracture planes are maintained at the incisal surfaces of the rods (solid black lines), where rod-interrrod continuity is limited, but the apical surfaces of the rods blend into a continuum with interrod.

Biomechanical Organization, Fracture Mechanics

The fracture toughness of human enamel was approximately three times greater than that of its major component, crystalline

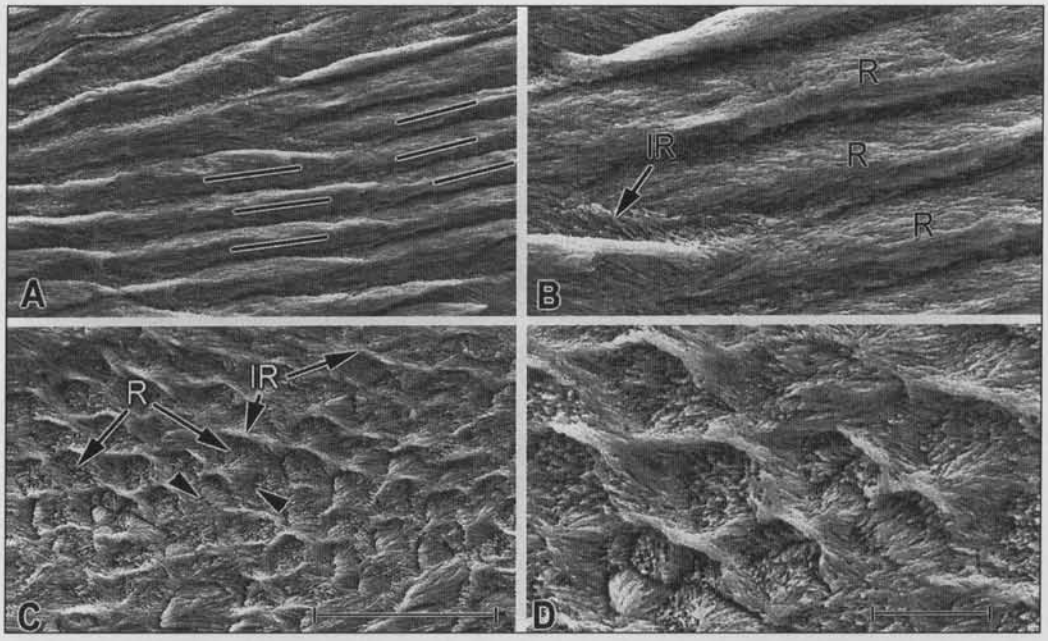

Figure 3. SEMs showing human rods in long-section (**A** & **B**) and in cross-section (**C** & **D**). Rods (R) are composed of bundles of crystallites, and interrod (IR) is composed of sheets of crystallites. The small angle of decussation between adjacent layers of rods is indicated by lines in **A** (bar = 20 μm). At higher magnification in **B** (bar = 5 μm), the continuity of rod with interrod can be seen. Panels **C** (bar = 20 μm) and **D** (bar = 5 μm) show the continuous waving "honeycomb" sheet of interrod, and the partial continuity of rod and interrod. Although some parts of individual rod boundaries appear clearly defined, other parts of the boundary of the same rod cannot be distinguished from interrod (**A-D**).

Hap (Table). Thus, biological processing is critical to the formation of tough enamel from weak Hap crystallites.

Although the along- and across-rod fracture toughnesses were statistically different (t statistic, -6.6; $p < 0.05$), the enamel was only 1.4 times tougher when measured across the rods as compared with the perpendicular direction along the rods. Anisotropy was present, but the effect of rod orientation was small. This suggests that many crystallites are oriented in a plane differing substantially from that of the main rod direction, and/or that rods have substantial sideways connections to their neighboring rods. Enamel clearly possesses mechanisms that limit crack growth along (parallel to) rods.

The geologic apatite crystals were approximately 1.8 times harder than human enamel (Table). This finding indicates that the minor components of enamel, protein and water, have a profound softening or plasticizing effect.

Little difference was found in toughness and hardness between the geologic Hap and fluorapatite crystals, suggesting that ion substitution did not markedly affect these parameters under the circumstances tested.

DISCUSSION

Biofabrication, Histology

The asymmetric shape of the Tomes' process and orientations of the rod and interrod secretory sites (Fig. 2) play an important role in matrix organization (Warshawsky *et al.*, 1981; Nanci and Warshawsky, 1984). The earliest matrix forms circumferentially to the Tomes' processes and largely represents interrod (Fig. 2). The later central matrix forms at the trailing basal tip of the Tomes' process and largely represents rod. The incisal edges of the proteinaceous matrix and its adjacent sides largely maintain their integrity, remaining distinct from adjacent proteinaceous matrices, but the trailing apical edges become much less distinct, intermingling with adjacent matrices (Boyde, 1987). Hence, during subsequent mineralization, the dominant incisal rod boundaries are preserved, but an interconnected structure is formed through the apical edges to create a continuum.

Spatial Organization, SEM

Ameloblasts in the incisal area migrate both outwardly and incisally (Figs. 1-3). Additionally, alternating cohorts of ameloblasts have a preference to migrate medially or distally to the direct radial path (Fig. 1) (Hanaizumi *et al.*, 1998). As each ameloblast migrates outward from the dentino-enamel junction to the outer surface of the tooth, it leaves an oriented columnar extrusion of proteinaceous matrix in its wake (Risnes, 1998; Smith, 1998). The vectors of movement of the ameloblasts and the temporal relationships among ameloblasts allow for interweaving among columns of matrix as well as specific connections to form between adjacent columns. Thus, the migratory paths of the ameloblasts and the orientations of the secretory sites of the Tomes' process orient the proteinaceous matrices, which in turn orient crystallite growth.

Continuity between rod and interrod is shown in Figs. 2E and 3. Other prior investigators, notably Boyde, have also noted continuity among enamel rods (Helmcke, 1967; Boyde, 1987). Continuity is also consistent with many prior SEMs, which typically show "fish scale"-shaped cross-sections of rods (Helmcke, 1967; Hu *et al.*, 1997; Warshawsky *et al.*, 1981; Risnes, 1998). The incisal part and sides of the "fish scale" are typically rounded and clearly defined, corresponding with the incisal edge and lateral sides of the extruded cylinder of proteinaceous matrix. In contrast, the apical part of the "fish scale" is often less clearly defined and appears to fade into interrod or to be squeezed between rods from the next row. This diffuse part of the "fish scale" represents the apical extent of the column of proteinaceous matrix, and it connects rods to interrod, forming a continuous meshwork (Figs. 2, 3).

Small fibers or sheets of interrod crystallites, running across rods, are shown in Figs. 1-3. We find that the angle between the dominant crystallite orientations in rod and interrod is approximately 60° in this plane (Figs. 1-3). The presence of interrod has been shown to be pronounced at the locations of cross-striations (Shellis, 1996). Boyde (1987) has previously suggested that cross-striations represent changes in the ratio of rod to interrod. We suggest that cross-striations are localized areas where spatial and temporal relationships among adjacent ameloblasts have allowed proportionally more interrod to develop.

The presence of continuity between rod and interrod and cross-striations, discerned by SEM, is consistent with the extraordinary toughness of enamel and its limited anisotropy, as measured by the fracture mechanics technique.

We acknowledge that the images in this study are two-dimensional and are limited to sagittal and face-on views in the area described in Fig. 1A.

Biomechanical Organization, Fracture Mechanics

Biological processing forms human enamel that is approximately 3 times tougher than its major component, crystalline Hap (Table). This large difference cannot be accounted for by differences due to impurities or ionic substitutions between dental Hap and geological apatites (Clark, 1966; Yoon and Newham, 1969; Ashby, 1993; Lawn, 1993).

Enamel was tougher in an across-rod direction than in an along-rod direction (Table), but the difference was smaller than previously believed (Rasmussen *et al.*, 1976; Yettram *et al.*, 1976; Hassan *et al.*, 1981; Spears *et al.*, 1993; Xu *et al.*, 1998). Enamel is only modestly anisotopic. The amount of anisotropy reflects a balance between protecting enamel from the most common functional stresses, as well as protecting it from less commonly directed functional or accidental stresses and orienting the dominant rods so as to reduce wear (Boyde, 1997). Some anisotropy may help to direct stresses away from brittle enamel to the resilient underlying dentin (Spears *et al.*, 1993; White *et al.*, 2000). Hence, it would not be surprising if different amounts of anisotropy were found in different parts of the coronal enamel structure (Xu *et al.*, 1998).

Protein remnants help to define the rounded discontinuity seen around the top of the "fish scale" on etched rods viewed in cross-section, as well as the linear demarcations between rods viewed in long-section (Figs. 2, 3). Almost all of the proteinaceous matrix is removed during mineralization and maturation (Robinson *et al.*, 1971; Wright *et al.*, 1997; Smith, 1998). However, some protein, notably ameloblastin, is retained, primarily at the incisal edges and proximal sides of rod boundaries (Hu *et al.*, 1997). The retention of ameloblastin in the sheath space may be due to its lack of interaction with other enamel proteins, especially amelogenin (Paine *et al.*, 1998).

Although minimal protein remains, it may have a profound effect on the mechanical properties of complex composite bioceramics, as previously shown for nacre and sea urchin teeth (Robinson *et al.*, 1971; Sarikaya *et al.*, 1995; Wang, 1998). First, the proteinaceous remnants define three-dimensional cleavage planes (Boyde, 1997). Thus, cracks will be preferentially deflected along and follow these cleavage planes (Hassan *et al.*, 1981). This could prevent catastrophic fractures from advancing straight through enamel, but instead spread the damage laterally over a much larger volume. Second, the proteinaceous remnants could allow limited differential movement between adjacent rods. This concept of stress reduction by limited slippage is supported by the differences in hardness (Table) and in elastic modulus (Craig *et al.*, 1961; Yoon and Newham, 1969; Xu *et al.*, 1998) between enamel and hydroxyapatite crystals. Marked slippage probably primarily manifests during loading to limit damage and prevent catastrophic failure.

New Structural Model

The structure of mature enamel is a reflection of the organization of the proteinaceous matrix (Fincham *et al.*, 1995; Hu *et al.*, 1997; Risnes, 1998). The unique properties of the enamel proteins are postulated to control crystallite habit. We speculate that amelogenin nanospheres permit crystallite growth in preferred orientations, but that ameloblastin may inhibit crystallite growth.

Analysis of our data emphasizes the critical importance of the organization of individual Hap crystallites to form bulk enamel. According to our findings, we propose a new model of enamel microstructure, illustrated by the schematic diagram in Fig. 2D. This model is consistent with much prior structural and developmental data referenced above, and notably with prior three-dimensional studies or serial/multiple-section reconstructions (Helmcke, 1967; Warshawsky and Smith, 1971; Risnes, 1987). This model is limited to a mesoscale description of enamel organization and structure and does not describe the crystallography of individual crystallites.

ACKNOWLEDGMENTS

The generous gift of constructive criticism and guidance has been provided by our many colleagues, including Drs. A. Boyde, A. Fincham, W. Dollase, A. Nanci, J. Oldak, C. Smith, and R. Young. This work was supported by the National Institutes of Health, National Institute of Dental and Craniofacial Research, under Grant Nos. DE12420, DE06988, DE13045, and DE11704.

REFERENCES

Ashby MF (1993). Materials selection in mechanical design. New York: Pergamon Press, p. 36.

Boyde A (1979). Carbonate concentration, crystal centers, core dissolution, caries, cross striations, circadian rhythms, and compositional contrast in the SEM. In: Tooth enamel III. Proceedings of the Third International Symposium on Tooth Enamel, its Development, Structure, and Composition. Nylen MU, Termine JD, editors. *J Dent Res* 58(Spec Iss B):981-983.

Boyde A (1987). A 3-D model of enamel development at the scale of one inch to the micron. *Adv Dent Res* 1:135-140.

Boyde A (1997). Microstructure of enamel. In: Ciba Foundation Symposium 205, Dental Enamel. Chadwick DJ, Cardew G, editors. New York: Wiley, pp. 18-31.

Clark SP Jr, editor (1966). Memorandum 97. Handbook of physical constants. New York: Geological Society of America.

Craig RG, Peyton FA, Johnson W (1961). Compressive properties of enamel, dental cements, and gold. *J Dent Res* 40:936-943.

Fincham AG, Moradian-Oldak J, Diekwisch TG, Lyaruu DM, Wright JT, Bringas P Jr, *et al.* (1995). Evidence for amelogenin "nanospheres" as functional components of secretory-stage enamel matrix. *J Struct Biol* 115:50-59.

Hanaizumi Y, Kawano Y, Ohshima H, Hoshino M, Takeuchi K, Maeda T (1998). Three dimensional direction and interrelationship of prisms in cuspal and cervical enamel of dog tooth. *Anat Rec* 252:355-368.

Hassan R, Caputo AA, Bunshaw RF (1981). Fracture toughness of human enamel. *J Dent Res* 60:820-827.

Helmcke J-G (1967). Ultrastructure of enamel. In: Structural and

chemical organization of teeth. Vol. II. Miles AEW, editor. New York: Academic Press, pp. 135-163.

Hu CC, Fukae M, Uchida T, Qian Q, Zhang CH, Ryu OH, *et al.* (1997). Sheathlin: cloning, cDNA/polypeptide sequences, and immunolocalization of porcine enamel sheath proteins. *J Dent Res* 76:648-657.

Lawn B (1993). Fracture of brittle solids. 2nd ed. Cambridge: Cambridge University Press, p. 55.

Lowenstam HA, Weiner S (1989). On biomineralization. New York: Oxford University Press, p. 175.

Nanci A, Warshawsky H (1984). Characterization of putative secretory sites on ameloblasts of the rat incisor. *Am J Anat* 171:163-189.

Paine ML, Krebsbach PH, Chen LS, Paine CT, Yamada Y, Deutsch D, *et al.* (1998). Protein-to-protein interactions: criteria defining the assembly of the enamel organic matrix. *J Dent Res* 77:496-502.

Rasmussen ST, Patchin RE, Scott DB, Heuer AH (1976). Fracture properties of human enamel and dentin. *J Dent Res* 55:154-164.

Risnes (1987). Multiplane sectioning and scanning electron microscopy as a method for studying the three-dimensional structure of mature dental enamel. *Scanning Microsc* 1:1893-1902.

Risnes S (1998). Growth tracks in dental enamel. *J Human Evol* 35:331-350.

Robinson C, Weatherell JA, Hallsworth AS (1971). Variation in composition of dental enamel within thin ground tooth sections. *Caries Res* 5:44-57.

Sarikaya M, Liu J, Aksay IA (1995). Nacre: properties, crystallography, morphology, and formation. In: Biomimetics design and processing of materials. Sarikaya M, Aksay IA, editors. New York: American Institute of Physics.

Shellis RP (1996). A scanning electron-microscopic study of solubility variations in human enamel and dentine. *Arch Oral Biol* 41:473-484.

Smith CE (1998). Cellular and chemical events during enamel maturation. *Crit Rev Oral Biol Med* 9:128-161.

Spears IR, van Noort R, Crompton RH, Cardew GE, Howard IC (1993). The effects of enamel anisotropy on the distribution of stress in a tooth. *J Dent Res* 72:1526-1531.

Wang R (1998). Fracture toughness and interfacial design of a biological fiber-matrix ceramic composite in sea urchin teeth. *J Am Ceram Soc* 81:1037-1040.

Warshawsky H, Smith CE (1971). A three-dimensional reconstruction of the rods in rat maxillary incisor enamel. *Anat Rec* 169:585-591.

Warshawsky H, Josephsen K, Thylstrup A, Fejerskov O (1981). The development of enamel structure in rat incisors as compared to the teeth of monkey and man. *Anat Rec* 200:371-399.

White SN, Paine ML, Luo W, Sarikaya M, Fong H, Yu Z, *et al.* (2000). The dentino-enamel junction is broad transitional zone uniting dissimilar bioceramic composites. *J Am Ceram Soc* 83:238-240.

Wright JT, Hall K, Yamauchi M (1997). The protein composition of normal and developmentally defective enamel. In: Ciba Foundation Symposium 205, Dental Enamel. Chadwick DJ, Cardew G, editors. New York: Wiley, pp. 85-106.

Xu HH, Smith DT, Jahanmir S, Romberg E, Kelly JR, Thompson VP, *et al.* (1998). Indentation damage and mechanical properties of human enamel and dentin. *J Dent Res* 77:472-480.

Yettram AL, Wright KWJ, Pickard HM (1976). Finite element stress analysis of the crowns of normal and restored teeth. *J Dent Res* 55:1004-1011.

Yoon HS, Newham RE (1969). Elastic properties of fluorapatite. *Am Miner* 54:1193-1197.